
Practical and sample efficient zero-shot HPO

Fela Winkelmolen
Amazon
<firstlastname>@gmail.com

Nikita Ivkin
Amazon
ivkin@amazon.com

H. Furkan Bozkurt
Amazon
bozkurh@amazon.com

Zohar Karnin
Amazon
zkarnin@amazon.com

Abstract

Zero-shot hyperparameter optimization (HPO) is a simple yet effective use of transfer learning for constructing a small list of hyperparameter (HP) configurations that complement each other. That is to say, for any given dataset, at least one of them is expected to perform well. Current techniques for obtaining this list are computationally expensive as they rely on running training jobs on a diverse collection of datasets and a large collection of randomly drawn HPs. This cost is especially problematic in environments where the space of HPs is regularly changing due to new algorithm versions, or changing architectures of deep networks. We provide an overview of available approaches and introduce two novel techniques to handle the problem. The first is based on a surrogate model and adaptively chooses pairs of dataset, configuration to query. The second, for settings where finding, tuning and testing a surrogate model is problematic, is a multi-fidelity technique combining HyperBand with submodular optimization. We benchmark our methods experimentally on five tasks (XGBoost, LightGBM, CatBoost, MLP and AutoML) and show significant improvement in accuracy compared to standard zero-shot HPO with the same training budget. In addition to contributing new algorithms, we provide an extensive study of the zero-shot HPO technique resulting in (1) default hyper-parameters for popular algorithms that would benefit the community using them, (2) massive lookup tables to further the research of hyper-parameter tuning.

1 Introduction

Hyperparameter (HP) tuning can be described as a blackbox optimization problem, where the goal is to minimize an expensive to evaluate blackbox function $\ell : \Theta \rightarrow \mathbb{R}$, with ℓ mapping a HP configuration $\theta \in \Theta$ to its generalization loss $\ell(\theta)$, and Θ representing the configuration search space. Typically we do not have access to gradient information and desire evaluating ℓ a small number of times, as each evaluation corresponds to a costly training of a machine learning model.

Most state-of-the-art HPO tools such as SMAC (Hutter et al., 2010), ParamILS (Hutter et al., 2009) and BOHB (Falkner et al., 2018) use Bayesian Optimization (BO) as the core component of their algorithms, where the blackbox function ℓ is modelled by a probabilistic surrogate model. After each evaluation, the returned value is incorporated into the surrogate model, which is then used to determine the next HP configuration to evaluate.

This approach has room for improvement in two aspects. First, if the surrogate model is trained from scratch, this leads to poor behavior in the initial stages, where not much is learned, and we are essentially querying random configurations. This is a problem either when the HPO budget, meaning

the number of evaluations of ℓ , is low, or when the HP space Θ is very rich, and it takes time to learn a reasonable surrogate for ℓ . The second issue is that the BO approach is by definition sequential; this poses a problem when we wish to speed up the HPO process by using multiple machines. Although there are several adaptations of BO in the literature aimed to solve both of these issues, zero-shot HPO is a natural fit to address both. It requires learning a set of HP configurations offline based on a meta-collection of datasets, thus taking advantage of external information. Furthermore, by having a pre-determined set of configurations, the HPO procedure becomes embarrassingly parallel.

To obtain the set of configurations, previous papers (Wistuba et al., 2015a,b; Pfisterer et al., 2018) run an offline meta-training job of the following nature. Given a collection of D datasets, choose N configurations and evaluate them on all D datasets. Configurations are picked at random or according to some heuristic such as *eps-net*. This offline process produces a performance table, i, j entry of which represents the loss of i -th configuration on j -th dataset. This performance table is used to find a set of K configurations that jointly minimize the aggregated loss over the whole dataset collection. In order to aggregate the losses over the datasets, it is common to normalize the scores and minimize the average normalized score.

Notice that the offline procedure evaluates the function ℓ at ND points, meaning it requires ND training jobs. This might seem reasonable because it is a one-time procedure. However, we claim that that a more efficient procedure would be highly beneficial. First, algorithms have new versions with new hyper-parameters being introduced; the magnitude of the change in the ℓ function and training time is particularly prohibitive when deep networks are involved. Second, even for a one-time job, the budget is limited, meaning that we have to compromise on our choice of number of datasets D or configurations N . In our experiments we verify that zero-shot HPO works better as we grow the number of datasets and the number of considered configurations.

To address this cost issue we design two solutions. The first is based on a surrogate function. The high level idea is that given the performance of several i, j pairs, we can estimate the performance of new pairs. We design an adaptive method for selecting i, j pairs to query while learning this surrogate function. This approach, called Offline Bayesian Optimization (OBO), adapts Bayesian optimization techniques to the non-standard optimization problem aimed at finding a set of HP configurations rather than an individual configuration.

Although this method performs well, there is a non-trivial cost to it. Choosing the right surrogate model, and tuning it correctly involves a certain amount of manual labor, especially given that we have to do that as we query the i, j pairs. In cases where this manual labor cannot be done, or a surrogate model is simply not good enough due to a particularly rich HP space, we provide a second solution. This second approach consists of a novel multi-fidelity algorithm solving the offline subset selection problem in a budget-efficient way. We evaluate both approaches in Section 8, demonstrating that their tradeoff of offline training budget B vs. overall accuracy is superior to existing baselines.

All our experiments are conducted based on tables that we pre-computed for 5 machine learning problems, for a total of over 6 million training jobs. These tables and analysis done with them are worthy on their own. First, by publishing their content we hope to make HPO research more approachable to the scientific community. Second, the zero-shot configurations found by our experiments can be used to greatly improve the performance vs. run-time tradeoff for the algorithms considered in our study.

Another contribution, interesting on its own right, is that of the normalized score. Despite the abundance of papers evaluating a technique on multiple datasets, we find it surprising that there is no real standard for a normalized score allowing to aggregate an algorithm’s performance across tasks. In Section 6 we formulate wanted properties of a normalized score. We review existing choices found in related literature and find that they do not have all of the wanted properties. For this reason we propose a normalized score called Relative Error Difference (RED), that obtains all needed properties.

2 Related work

A number of previous works attempt to use evaluations of related tasks to speed up BO. Feurer et al. (2015) and Brazdil et al. (2003) propose to start the search from configurations that performed well on similar datasets and accomplish this by computing a distance metric on meta-data of the datasets. Although the results presented in the papers are positive, it is not always clear how to

collect meta-data, which explicit meta-data features would be useful, and how to automatically get the correct distance metric relevant to the specific setting being solved.

Wistuba et al. (2015a) are the first to frame zero-shot HPO as an optimization problem minimizing the meta-loss over a collection of datasets. The HPs found this way are proposed as an initialization strategy for BO. Differentiable surrogate models are used to decrease the required evaluations on the meta-datasets. This, in combination with a discrete relaxation of the minimization problem, allows the authors to optimize the meta-loss using gradient descent. They show that using this initialization strategy followed by standard single task BO methods matches the performance of state-of-the-art meta-learning algorithms, as well as initialization strategies that make use of meta-data based distances.

In a second paper (Wistuba et al., 2015b), the same authors use a greedy incremental algorithm to find a set of zero-shot HPO configurations, giving similar results. In this case, a full grid search is performed on all datasets, thus not requiring any surrogate model. Pfisterer et al. (2018) frame the zero-shot HPO problem as one of finding multiple default configurations. They combine both of the above ideas, by limiting the search space to a discrete set of random configurations (as opposed to the grid search used in (Wistuba et al., 2015b)) and use an iterative greedy algorithm for finding a sequence of zero-shot configurations, but use a surrogate model for evaluations. They do not provide details about neither the type of surrogate model nor the amount of savings it brought.

Similar ideas have been applied to other use cases. In particular, Feurer et al. (2015) use zero-shot HPO to select a portfolio of machine learning pipelines, while Lindauer & Hutter (2018) applies similar approaches to optimizing the configuration of SAT solvers. Finally, in van Rijn et al. (2018) each learned zero-shot hyperparameter is a function of the dataset meta-data, instead of being a fixed configuration. Perrone et al. (2019) make use of related tasks in order to limit the search space, rather than finding a small set of HP configurations. Specifically, they use the related tasks to eliminate regions of the search space that are very likely to provide poor results.

A different line of work attempts to use the evaluations of related tasks directly in the modeling of the surrogate function (Yogatama & Mann, 2014; Perrone et al., 2018). However, developing modeling techniques that robustly and effectively apply transfer learning on real-world tasks has proven challenging, and thus is still an area under active research. See chapter 2 of Hutter et al. (2019) for a broader review of such transfer learning techniques. We note that (1) our technique is quite different and likely complementary to that line of work, and (2) these works provide outside information, but the problem of parallelism remains.

3 Zero-shot HPO

Algorithm 1: Naive greedy algorithm

Input: number of desired zero-shot configurations K ,
search space Θ containing N configurations $\theta_1, \dots, \theta_N$
Output: $S \in [N]^K$, indices of found zero-shot configurations
for $j = 1, 2, \dots, K$ **do**
| set $S_j = \arg \min_{i \in [N]} L(\{S_1, \dots, S_{j-1}, i\})$
end

Let us start by describing the computationally efficient greedy algorithm used by previous works. We will call this baseline Naive. We are given a collection of D datasets, and a (possibly infinite) collection Θ of configurations. In the naive approach, we select N configurations $\theta_1, \dots, \theta_N \in \Theta$ by i.i.d copies from a manually defined distribution. The amount of configurations N is chosen according to the overall budget of training jobs. In this method we will invoke ND training jobs, meaning that for a budget of B we set $N = \lfloor B/D \rfloor$.

We will use $[N]$ as a shorthand for the set of integers $\{1, 2, \dots, N\}$. For each configuration θ and dataset d , we run a training job to compute the validation loss $\ell(d, \theta)$. Given these values, we run an

optimization procedure finding K configurations $S \in [N]^K$ that jointly obtain the best performance on the dataset collection, by minimizing the following zero-shot meta-loss

$$L(S) = D^{-1} \sum_{d=1}^D \min_{i \in S} \{\ell(d, \theta_i)\} \quad (1)$$

Finding the optimal subset of size K is known to be NP-hard. This was already pointed out in Pfisterer et al. (2018). Fortunately, there is a very simple approximation algorithm using the greedy approach. First, we show that L is monotone decreasing and supermodular. The proof of this lemma and the Theorem below is available in Appendix B.

Lemma 1. *The function L defined in Equation 1 is monotone decreasing, i.e. $\forall A$ and $j \notin A$: $L(A \cup \{j\}) \leq L(A)$ and super-modular:*

$$\forall A \subseteq B \subset \mathbb{N} \text{ and } j \notin B : L(A) - L(A \cup \{j\}) \geq L(B) - L(B \cup \{j\}).$$

As a result of Lemma 1 we know, by Nemhauser et al. (1978), that the greedy solution aiming to minimize $L(S)$ provides a $(1 - e^{-1})$ -approximation to the optimal solution. For completeness, we provide an extension of this proof for the scenario where the local greedy step, i.e., the step finding the best configuration to add to the collection, is itself an approximation rather than an exact solution. This extension is useful for understanding the guarantees of methods that do not fill out the full $N \times D$ table.

Theorem 1. *A greedy algorithm making steps towards ϵ -approximates of best local improvements finds a $(1 - e^{-1+\epsilon})$ -approximation to the problem $\max_{|S| \leq k} L(S)$ for monotone increasing submodular L .*

4 Offline Bayesian optimization (OBO)

When a probabilistic surrogate is available, an efficient zero-shot algorithm can be obtained by applying Bayesian optimization to optimize our zero-shot meta-loss. This is a fully sequential procedure to select evaluations, where at each time t we select a candidate θ^t and a dataset d^t to evaluate. We define $\ell^t(d, \theta)$ to be equal to ∞ if the configurations has not yet been selected at time t , and equal to $\ell(d, \theta)$ otherwise. In the same vein, $L^t(S) = D^{-1} \sum_{d=1}^D \min_{i \in S} \{\ell^t(d, \theta_i)\}$, and at each time t the current best zero-shot configurations are denoted with $S^t = \arg \min_{S \in [N]^K} L^t(S)$. At each step t we train a probabilistic surrogate model $\mathcal{M}(\ell^t)$, that gives us a predictive distribution of ℓ . We thus proceed by iteratively running the following two steps: (1) select the most promising configuration θ^t , and its most promising location l^t , and (2) select the most promising dataset d^t to evaluate using the configuration θ^t at location l^t .

Formally, at step t we select the configuration θ^t and the location l^t such that substituting location l^t with θ^t and evaluating this configuration on all datasets brings the highest expected improvement, up to location l^t :

$$\theta^t, l^t = \arg \max_{\theta, l \in \Theta \times [K]} \mathbb{E}_{\ell \sim \mathcal{M}(\ell^t)} \frac{(\sum_{d=1}^D [\min_{i \in [l]} \ell^t(d, S_i^t) - \min(\ell(d, \theta), \min_{i \in [l-1]} \ell^t(d, S_i^t))])^+}{\sum_{d=1}^D \mathbb{1}(\ell^t(d, \theta) = \infty)}$$

Note that any new candidate configuration will perform well only when enough datasets have been evaluated with this configuration. For this reason, we estimate the performance of a candidate configuration if we were to evaluate it on *all* datasets. Otherwise we would never select new configurations. It is important to normalize by the number of remaining evaluations required to fully evaluate the configuration on all datasets. This way we select the configuration that maximizes the expected improvement *per training job*.

Next, we select the dataset with the highest expected decrease in loss up to l^t , if θ^t is selected as the l^t -th zero-shot configuration:

$$d^t = \arg \min_{d \in [D]} \mathbb{E}_{\ell \sim \mathcal{M}(\ell^t)} [\min(\ell(d, \theta^t), \min_{i \in [l^t-1]} \ell^t(d, S_i^t)) - \min(\ell^t(d, \theta^t), \min_{i \in [l^t-1]} \ell^t(d, S_i^t))]$$

The above expectation is computed through sampling. As we choose to optimize for a specific location, we do not need to compute the greedy procedure for each sample.

Choosing the surrogate model The first major decision regards the type of surrogate model. Here, although previous papers chose Gaussian Processes (GPs) we avoided this option since (1) our model must learn quickly (2) the hyper-parameter space can be quite rich, including categorical features that need special handling, and often conditional features that are known to interact poorly with GPs. For these reasons, in an attempt to obtain the best performing surrogate possible in our settings, we choose to use random forests as a surrogate model, as they have already been proven to work well on similar search spaces in Hutter et al. (2010). The second major decision regards the input to the surrogate model. We experimented with (1) a single surrogate model taking in the dataset id as an input (2) separate models for each dataset (3) a mixture, where a global model takes in the predictions of the dataset specific model as inputs. Since a long portion of the time is spent where many datasets have very little information, we found that the variations including local models, meaning surrogate models for specific datasets, are outperformed by the first option having a single global model.

5 Multi-fidelity (MF) zero-shot HPO

Let’s begin with the setting of $K = 1$. Here, the problem has a straightforward reduction to the best arm identification task in multi-armed bandits. A query to a configuration consists of selecting a random dataset and computing the loss $\ell(d, \theta)$. This is an unbiased estimator of the mean over all datasets. In our setting, we have a fixed budget of queries to ℓ . As such, a first attempt would be to use the techniques provided by Karnin et al. (2013) in their “successive halving” algorithm, proven to be highly efficient in the best arm identification task. Unfortunately, we have three added complications. First, we have a finite set of datasets, meaning that there is a maximum to the number of arm pulls. Second, when choosing an aggregation function other than mean, the confidence bounds become less trivial. This is mitigated by the analysis of Jamieson & Talwalkar (2016), showing that the successive halving algorithm works well as the estimates converge to a single value, and there is no need for the algorithm to be aware of the convergence bound. Lastly, the number N of possible configurations θ is not pre-determined as we can choose to explore either many configurations in a shallow manner or a few but exhaustively. This is exactly the problem dealt with by HyperBand (Li et al., 2017), where they build upon the successive halving algorithm.

We conclude that for the setting of $K = 1$ the problem fits the framework of HyperBand (HB) exactly. Therefore we can use either HB or an extension of it, making use of surrogate functions such as BOHB (Falkner et al., 2018). This solution for $K = 1$ suggests a solution for $K > 1$, where we aim to find a set S of K configurations. We use the term *location* for a chosen item in S to denote its location in the sequential greedy process. With this term, the algorithm chooses the item in location 1 based on the ℓ values, then chooses an item for location 2 based on its improvement over the ℓ value already achieved by location 1. It moves on to the other locations sequentially in the same way it handled location 2. We get an approximately optimal configuration for each location, thus by Theorem 1 we get $(1 + e^{-1+\epsilon})$ approximation to the optimal subset S of size K .

Although this method is sensible at a high level there are a few key issues to be dealt with, that require a non-trivial solution.

Noise reduction: When comparing two configurations based on a subset of the datasets of equal sizes we make sure the subsets contain the same datasets. This removes some variance from the estimates. To that end, we pick a single random shuffling of the datasets, and a query of configuration θ with resource r means computing its loss on the first r datasets and computing the mean. The same random order is used throughout the experiment

Information reuse: Consider a setting where we wish to evaluate the performance of a configuration θ as the second configuration in our set. If θ happened to perform well as a first element, we queried its performance on many datasets, and the evaluation actually comes for free. In general, when we start the process of discovering the configuration for location > 1 in the set, we already have information from previous locations. We design the HyperBand instance to reuse this information.

Resource Balancing: It is unclear how we should balance the resources among the K locations. Realistically, most of the value comes from the first locations. This can be made formal by noticing the magnitude of the losses and their variances become smaller as the location grows. As the magnitude

of the loss shrinks, the benefit from minimizing it decreases, therefore the resources to locations with smaller losses can be smaller.

The issue of resource balancing brings a major challenge. If we only start exploring location j once we fixed locations $j' < j$, we cannot be adaptive. Moreover, even if we do not wish to be adaptive, by splitting the resources in advance, for example equally, we cannot control whether we end up actually using equal resources or, due to information reuse, end up with remaining resources and an unclear way to use them. The only straightforward way would be using them for the last location, but that is hardly a choice we would have done knowingly. To this end, we modify our HyperBand implementation in a way that allows exploring all locations simultaneously.

The closest previous work we are aware of is that of Streeter & Golovin (2009). The authors provide an online algorithm that sequentially selects different sets of size K and, on average, competes with the optimal set in hindsight. Their technique provably works for any monotone decreasing supermodular function. This is a slightly different setting as the objective is to minimize regret rather than identifying the best subset. In order to handle the fact that a change in location j changes the losses observed at locations $j' > j$, they require the algorithm for selecting each location to be very robust, and indeed they use EXP3.P (Auer et al., 2002), which is a multi-arm bandit algorithm for the regret setting, for adversarial realizations and a high probability guarantee. This algorithm is indeed robust enough to provide rigorous guarantees but not very practical for our setting. In particular, it is aimed for a regret guarantee rather than best arm identification.

Due to this, we use an asynchronous HyperBand algorithm (see Appendix C for a more detailed description) with the following modification: at each step, when selecting what job to promote from a specific rung, we independently select the location that we are targeting. This location will determine the losses, and thus what job will be promoted to the next rung. Thus, once the rung from which to promote is selected as usual, we select the new candidate to promote as analyzed in Algorithm 2. We first select a location l such that the resources used per locations follows our predetermined allocation. Then, among all candidates in the current rung that have not yet been promoted, we select the candidate that gives the lowest loss when appended to the current best $l - 1$ zero-shot candidates.

Algorithm 2: Anytime combinatorial HyperBand: candidate selection

Input: Set Θ of candidates in the current rung, resource ratio vector ρ , previous resources used for each location r

Output: Next candidate θ_{\min}

Let l_{\max} be the smallest location index whose HB instance does not have a candidate evaluated on all datasets, or 1 if no such index exists;

Let l be $\arg \min_{i \in [l_{\max}]} r_i \cdot \rho_i$;

Let $\theta_i, \dots, \theta_{l-1}$ be the $l - 1$ zero-shot configurations as computed using Algorithm 1 among all configurations already evaluated on all datasets;

Return $\arg \min_{\theta \in \Theta} \sum_{d=1}^{r_l} \min(\min_{i \in [l-1]} \ell(d, \theta_i), \ell(d, \theta))$;

6 Relative error difference (RED)

Zero-shot HPO can be used with any loss ℓ and any aggregate loss L . However, as we average losses computed over different datasets, one should be careful to choose a loss that can be meaningfully averaged across datasets.

The loss we use in our experiments is what we call *relative error difference* (RED), computed comparing to a reference loss r_d that we first compute for each dataset d . Thus, if $\ell(d, \theta)$ is an unnormalized error metric for dataset d , such as miss-classification rate, we normalize this metric by taking $\ell(d, \theta) = \text{RED}(\tilde{\ell}(d, \theta), r_d)$, where

$$\text{RED}(a, b) = \frac{a - b}{\max(a, b)}$$

here we assume $0/0$ to be equal to 0. As an example, if one dataset has a reference error rate of 40%, and a second dataset has a reference error rate of 4%, this metric considers a reduction of the former to 30% equivalent to a reduction of the latter to 3%. RED provides us with robust aggregation thanks

to its desirable properties compared to other normalization schemes, as described in more detail in Appendix A.

7 Experimental setup

Table 1: Size of pre-computed tables.

setting	num. datasets	num. configs	num. HPs	total training jobs
XGBoost	80	18 406	9	1 472 480
LightGBM	88	30 000	9	2 640 000
CatBoost	72	25 042	7	1 803 024
MLP	59	5 445	8	321 255
ZAML	40	3 555	32	142 200
total				6 378 959

We test our approach on four commonly used general purpose supervised learning algorithms (XGBoost (Chen & Guestrin, 2016), CatBoost (Prokhorenkova et al., 2018), LightGBM (Ke et al., 2017), and MLP) and ZAML, a zero-shot AutoML search space, see Appendix D for details. For each of the above algorithms we pre-compute the miss-classification rate for a large number of classification datasets using a large number of randomly sampled HP configurations. We make the content of tables publicly available, with the hope it will aid further research into AutoML and transfer learning¹. For each training we store the validation and test miss-classification rate, as well as the wall-clock time required to complete the training job. We also provide the exact HPs used for each configuration. All datasets used have at least 3000 rows and originate from publicly available repositories: Kaggle², OpenML (Vanschoren et al., 2013), UCI (Dua & Graff, 2017) and the AutoML Challenge (Guyon et al., 2019). Minimal standard preprocessing, such as TF-IDF and one hot encoding, were applied to transform the input into purely numeric matrices. To assure high generalization accuracy estimates, we use .5/.25/.25 sized splits for training, validation and test sets, respectively. The exact size of the tables and the number of HPs is listed in Table 1. In the ZAML setting, we include the choice of feature processing and algorithm selection in the search space. Thus each configurations specifies the type of feature processing used, the HPs for the feature processors selected, the machine learning algorithm to use and the HPs of this algorithm. See Appendix D for a full description of all search spaces used.

In all our experiments our loss is the average RED. The unnormalized error metric we use is the miss-classification rate, and our reference metric is obtained by averaging the test metric of the 10 models with the lowest validation error in our discrete set of random configurations. To use the limited number of datasets efficiently we evaluate our method in a leave-one-dataset-out fashion: when computing the performance of zero-shot configurations on any given datasets we use all other datasets as source tasks. We always report the *test metric* of the hyperparameter configuration with the best *validation error* up to any given number of evaluations.

We evaluate the following four algorithms, all with a budget of 3000 training jobs:

Naive: The baseline defined in Algorithm 1.

Surrogate: Both Wistuba et al. (2015a) and Pfisterer et al. (2018) make use of surrogates trained on each dataset, to predict the performance of previously unseen configurations. The same considerations made in Section 4 for selecting the surrogate of OBO apply, thus we experimented with the same surrogate models. In addition, we attempted to use XGBoost instead of a random forest and use 1000 trees in the joint models instead of the default 100. The best performing surrogate, used for all further experiments, ended up being Scikit-learn’s (Pedregosa et al., 2011) random forest with default HPs, with one surrogate trained per dataset.

OBO: The BO approach of Section 4. In our experiment this surrogate model is a random forest with 20 trees. We consider the predictions from the single trees to be an approximation to taking 20 samples from the posterior distribution. This is similar to what is done in SMAC (Hutter et al., 2010)

¹Link will be made available in future versions

²<https://kaggle.com>

for standard Bayesian optimization. As with **Surrogate**, we used the default parameters provided by sklearn in order to avoid overfitting to our tables.

MF: The multi-fidelity approach described in Section 5.

We note that all preliminary comparisons for choosing the surrogate model were made on the XGBoost and MLP tables alone, while in all other settings we ran only the final version of the algorithms. This drastically reduces the chances that we suffered from overfitting to our experimental settings.

8 Results

Our experiments show that the two algorithms proposed clearly outperform existing baselines. In table 2 we can see that OBO consistently outperforms the Surrogate baseline. Similarly, as shown in Table 3, if a simpler method without surrogate is preferred, our multi-fidelity algorithm proves superior to the existing Naive approach used in previous works. Note that both tables display the RED between the given method and the baseline this method is compared to, as this is the most accurate way to compare two methods, yielding the most statistical power. In Appendix G we provide additional figures with comparisons to random search Bergstra & Bengio (2012), the online HPO technique that best competes with zero-shot HPO in terms of simplicity and parallelism. There we can see that random search requires a 10 to 50 times higher budget to match the performance of zero-shot HPO. In the same appendix, we also provide additional results showing that in most settings OBO outperformed MF, however this gap disappeared for ZAML. Our conjecture is that when the search space becomes more complex and harder to model the benefit of a surrogate model disappears, an argument in favour of MF in these settings.

We hope that methods described, the zero-shot configurations published, and the tables we released will all help machine learning practitioners reach state-of-the-art model performance more quickly, freeing them from some of the costly and time consuming hyperparameter tuning effort normally required.

Table 2: OBO (vs Surrogate) – avg RED (\pm std. err.) – lower is better.

	1 zero-shot config	2 zero-shot configs	5 zero-shot configs
XGBoost	-5.34% (\pm 1.17)	-5.07% (\pm 1.01)	-2.94% (\pm 0.92)
LightGBM	-0.74% (\pm 0.57)	-1.25% (\pm 0.58)	-0.94% (\pm 0.54)
CatBoost	-2.48% (\pm 1.55)	-1.69% (\pm 1.54)	-2.83% (\pm 1.58)
MLP	-9.09% (\pm 2.94)	-4.30% (\pm 1.54)	-1.60% (\pm 1.55)
ZAML	-1.24% (\pm 2.70)	-1.67% (\pm 3.07)	-0.62% (\pm 2.23)
Combined	-3.71% (\pm 0.77)	-2.82% (\pm 0.63)	-1.89% (\pm 0.57)

Table 3: MF (vs Naive) – avg RED (\pm std. err.) – lower is better.

	1 zero-shot config	2 zero-shot configs	5 zero-shot configs
XGBoost	-5.19% (\pm 1.75)	-5.66% (\pm 1.72)	-4.64% (\pm 1.71)
LightGBM	-4.68% (\pm 1.40)	-3.95% (\pm 1.45)	-4.16% (\pm 1.42)
CatBoost	+1.22% (\pm 0.87)	+0.56% (\pm 1.02)	+0.78% (\pm 0.99)
MLP	-1.22% (\pm 1.53)	-2.50% (\pm 1.17)	-1.81% (\pm 1.02)
ZAML	-0.43% (\pm 3.50)	-2.43% (\pm 3.70)	-0.95% (\pm 3.69)
Combined	-2.44% (\pm 0.77)	-2.96% (\pm 0.77)	-2.44% (\pm 0.76)

Broader Impact

There has been a recent trend towards exponential growth in the compute resources required to obtain state-of-the-art results in machine learning³, making research in some subfields prohibitively expensive. Though in general zero-shot HPO might benefit those with the resources to perform a expensive one-off offline optimization procedures, everyone can use the configurations computed with these techniques, assuming they are built for a publicly available algorithm. While on the one hand our work might increase the visibility and use of zero-shot HPO techniques, and this line of research might benefit those with access to massive computational resources, on the other hand this paper democratizes zero-shot HPO in three important ways: (1) reducing this offline cost, by providing two algorithm both explicitly aimed at reducing the cost of computing zero-shot HPO configurations (2), providing already computed zero-shot configurations for everyone to use on a selection of popular public algorithms, greatly reducing the difficulty and cost for practitioners to perform HPO, and (3) providing tables of pre-computed training results that can be used by researchers to benchmark new HPO techniques without requiring prohibitive computational budgets.

References

- Peter Auer, Nicolo Cesa-Bianchi, Yoav Freund, and Robert E Schapire. The nonstochastic multiarmed bandit problem. *SIAM journal on computing*, 32(1):48–77, 2002.
- James Bergstra and Yoshua Bengio. Random search for hyper-parameter optimization. *Journal of machine learning research*, 13(Feb):281–305, 2012.
- Pavel B Brazdil, Carlos Soares, and Joaquim Pinto Da Costa. Ranking learning algorithms: Using ibl and meta-learning on accuracy and time results. *Machine Learning*, 50(3):251–277, 2003.
- Tianqi Chen and Carlos Guestrin. Xgboost: A scalable tree boosting system. In *Proceedings of the 22nd acm sigkdd international conference on knowledge discovery and data mining*, pp. 785–794, 2016.
- Dheeru Dua and Casey Graff. UCI machine learning repository, 2017. URL <http://archive.ics.uci.edu/ml>.
- Stefan Falkner, Aaron Klein, and Frank Hutter. Bohb: Robust and efficient hyperparameter optimization at scale. *arXiv preprint arXiv:1807.01774*, 2018.
- Matthias Feurer, Jost Tobias Springenberg, and Frank Hutter. Initializing bayesian hyperparameter optimization via meta-learning. In *Twenty-Ninth AAAI Conference on Artificial Intelligence*, 2015.
- Isabelle Guyon, Lisheng Sun-Hosoya, Marc Boullé, Hugo Jair Escalante, Sergio Escalera, Zhengying Liu, Damir Jajetic, Bisakha Ray, Mehreen Saeed, Michéle Sebag, Alexander Statnikov, WeiWei Tu, and Evelyne Viegas. Analysis of the automl challenge series 2015-2018. In *AutoML*, Springer series on Challenges in Machine Learning, 2019. URL <https://www.automl.org/wp-content/uploads/2018/09/chapter10-challenge.pdf>.
- F Hutter, L Kotthoff, and J Vanschoren. Automl: methods, systems, challenges (2018). *Book in preparation. Current draft at <https://www.automl.org/book/>. Accessed July, 2019.*
- Frank Hutter, Holger H Hoos, Kevin Leyton-Brown, and Thomas Stützle. Paramils: an automatic algorithm configuration framework. *Journal of Artificial Intelligence Research*, 36:267–306, 2009.
- Frank Hutter, Holger H Hoos, and Kevin Leyton-Brown. Sequential model-based optimization for general algorithm configuration (extended version). *Technical Report TR-2010-10, University of British Columbia, Computer Science, Tech. Rep.*, 2010.
- Kevin Jamieson and Ameet Talwalkar. Non-stochastic best arm identification and hyperparameter optimization. In *Artificial Intelligence and Statistics*, pp. 240–248, 2016.
- Zohar Karnin, Tomer Koren, and Oren Somekh. Almost optimal exploration in multi-armed bandits. In *International Conference on Machine Learning*, pp. 1238–1246, 2013.

³<https://openai.com/blog/ai-and-compute/>

- Guolin Ke, Qi Meng, Thomas Finley, Taifeng Wang, Wei Chen, Weidong Ma, Qiwei Ye, and Tie-Yan Liu. Lightgbm: A highly efficient gradient boosting decision tree. In *Advances in neural information processing systems*, pp. 3146–3154, 2017.
- Liam Li, Kevin Jamieson, Afshin Rostamizadeh, Ekaterina Gonina, Moritz Hardt, Benjamin Recht, and Ameet Talwalkar. Massively parallel hyperparameter tuning. *arXiv preprint arXiv:1810.05934*, 2018.
- Lisha Li, Kevin Jamieson, Giulia DeSalvo, Afshin Rostamizadeh, and Ameet Talwalkar. Hyperband: A novel bandit-based approach to hyperparameter optimization. *The Journal of Machine Learning Research*, 18(1):6765–6816, 2017.
- Marius Lindauer and Frank Hutter. Warmstarting of model-based algorithm configuration. In *Thirty-Second AAAI Conference on Artificial Intelligence*, 2018.
- George L Nemhauser, Laurence A Wolsey, and Marshall L Fisher. An analysis of approximations for maximizing submodular set functions—i. *Mathematical programming*, 14(1):265–294, 1978.
- F. Pedregosa, G. Varoquaux, A. Gramfort, V. Michel, B. Thirion, O. Grisel, M. Blondel, P. Prettenhofer, R. Weiss, V. Dubourg, J. Vanderplas, A. Passos, D. Cournapeau, M. Brucher, M. Perrot, and E. Duchesnay. Scikit-learn: Machine learning in Python. *Journal of Machine Learning Research*, 12:2825–2830, 2011.
- Valerio Perrone, Rodolphe Jenatton, Matthias W Seeger, and Cédric Archambeau. Scalable hyperparameter transfer learning. In *Advances in Neural Information Processing Systems*, pp. 6845–6855, 2018.
- Valerio Perrone, Huibin Shen, Matthias W Seeger, Cedric Archambeau, and Rodolphe Jenatton. Learning search spaces for bayesian optimization: Another view of hyperparameter transfer learning. In *Advances in Neural Information Processing Systems*, pp. 12751–12761, 2019.
- Florian Pfisterer, Jan N van Rijn, Philipp Probst, Andreas Müller, and Bernd Bischl. Learning multiple defaults for machine learning algorithms. *arXiv preprint arXiv:1811.09409*, 2018.
- Liudmila Prokhorenkova, Gleb Gusev, Aleksandr Vorobev, Anna Veronika Dorogush, and Andrey Gulin. Catboost: unbiased boosting with categorical features. In *Advances in neural information processing systems*, pp. 6638–6648, 2018.
- Matthew Streeter and Daniel Golovin. An online algorithm for maximizing submodular functions. In *Advances in Neural Information Processing Systems*, pp. 1577–1584, 2009.
- Jan N van Rijn, Florian Pfisterer, Janek Thomas, Andreas Muller, Bernd Bischl, and Joaquin Vanschoren. Meta learning for defaults—symbolic defaults. In *Neural Information Processing Workshop on Meta-Learning*, 2018.
- Joaquin Vanschoren, Jan N. van Rijn, Bernd Bischl, and Luis Torgo. Openml: Networked science in machine learning. *SIGKDD Explorations*, 15(2):49–60, 2013. doi: 10.1145/2641190.2641198. URL <http://doi.acm.org/10.1145/2641190.2641198>.
- Martin Wistuba, Nicolas Schilling, and Lars Schmidt-Thieme. Learning hyperparameter optimization initializations. In *2015 IEEE international conference on data science and advanced analytics (DSAA)*, pp. 1–10. IEEE, 2015a.
- Martin Wistuba, Nicolas Schilling, and Lars Schmidt-Thieme. Sequential model-free hyperparameter tuning. In *2015 IEEE international conference on data mining*, pp. 1033–1038. IEEE, 2015b.
- Dani Yogatama and Gideon Mann. Efficient transfer learning method for automatic hyperparameter tuning. In *Artificial intelligence and statistics*, pp. 1077–1085, 2014.

A Comparison of RED to other metrics

In this section we motivate our use of RED as an objective when computing the zero-shot configurations, as well as when analyzing our results by aggregating the metric across multiple datasets. In particular, we motivate the use of RED over the following normalization schemes that have been used in the literature:

- **No normalization.** We denote the unnormalized miss-classification rate of the configuration θ on dataset d with $\tilde{\ell}(d, \theta)$.
- **Rank normalization.** The rank normalized score is defined as the rank among Θ , the set of all considered configurations, and can be normalized to be between 0 and 1:

$$\ell(d, \theta) = \frac{|\{\tilde{\theta} \in \Theta \mid \tilde{\ell}(d, \tilde{\theta}) < \tilde{\ell}(d, \theta)\}|}{|\Theta|}$$

- **Min-max normalization.** Linearly rescales the scores to keep the range between 0 and 1.
- **Stddev normalization.** Linearly rescales the scores to have mean zero and standard deviation one.
- **RED.** The relative error difference metric described in section 6.

Wistuba et al. (2015a) use min-max normalization, whereas in Wistuba et al. (2015b) min-max normalization is used only when evaluating the results, but rank normalization is used in the objective. And finally, Pfisterer et al. (2018) use stddev normalization.

It is not immediately obvious what the trade-offs of different metrics are. We thus looked at the following two properties that we deem important when averaging metrics across datasets, and show that only RED has both:

Robust to rescaling. When comparing metrics averaged over multiple datasets, without using any normalization, typically only the metrics with the largest range will meaningfully affect the results. While often the true utility of any improvement depends on the use case at hand, a desirable property—all other things being equal—is that a halving of the error metric always contributes the same value. Any of the normalization schemes described above, except for no normalization, are invariant under linear rescaling and thus have this property.

Robust to simple datasets. There are some datasets for which in fact we do not want the results to affect the aggregate metric. These are datasets where the performance of the best configurations is very similar to the performance of the worst configuration. It is important to note that here we are talking about similarity in relative terms, not absolute terms. Reducing the error rate from 0.1% to 0.001% can be very valuable and will likely require a much better model. Conversely, reducing an error rate from 32% to 31% is, in most cases, not as impressive. All normalization schemes except RED and no normalization will magnify any difference in the case where all configurations perform very closely for a specific dataset. Thus only RED fulfills both desired properties.

Table 4: Metric normalization comparison.

Normalization type	none	rank	stddev	min-max	RED
Robust to rescaling	no	yes	yes	yes	yes
Robust to simple datasets	yes	no	no	no	yes

Here we focused our discussion on the per dataset metric ℓ , such that the values from different datasets can be aggregated. For the aggregation itself we use the average, as this gives us a principled way to approximate the expected metric on new datasets. There are however two cases where it might be desirable to explore alternative aggregation functions. The first case is when we expect the new dataset to not come from (approximately) the same distribution as the meta datasets used to learn the zero-shot configurations. The second case is when we are not interested in the expected metric, for example if even in a single dataset the metric can vary by many orders of magnitude not proportional to the actual utility of the results. In such cases different aggregation functions such as median or P90 can be warranted. Our preliminary experiments (see Appendix G) however point towards the average to be a superior choice in our settings.

B Proofs

For simplicity we redefine D to be the set of all datasets.

Proof of Lemma 1. Let's first show that $L(S)$ is monotone decreasing. For any given A, j , and d :

$$\begin{aligned} L(A \cup \{j\}) &= \frac{1}{|D|} \sum_{d \in D} \min_{i \in A \cup \{j\}} \{\ell(d, \theta_i)\} \\ &= \frac{1}{|D|} \sum_{d \in D} \min\{\min_{i \in A} \{\ell(d, \theta_i)\}, \ell(d, \theta_j)\} \leq \frac{1}{|D|} \sum_{d \in D} \min_{i \in A} \{\ell(d, \theta_i)\} = L(A) \end{aligned}$$

Next, we will show that $L(S)$ is super-modular. Recall that submodularity is implied by

$$\forall A \subseteq B \subseteq \mathbb{N} \text{ and } j \notin B : L(A) - L(A \cup \{j\}) \geq L(B) - L(B \cup \{j\})$$

Given any A, B and j we can split the dataset collection D into three subsets such that $D = D_1 \cup D_2 \cup D_3$

$$\begin{aligned} D_1 &= \left\{ d \mid \ell(d, \theta_j) < \min_{i \in B} \{\ell(d, \theta_i)\} \right\}, \quad D_2 = \left\{ d \mid \min_{i \in B} \{\ell(d, \theta_i)\} \leq \ell(d, \theta_j) \leq \min_{i \in A} \{\ell(d, \theta_i)\} \right\} \\ D_3 &= \left\{ d \mid \ell(d, \theta_j) > \min_{i \in A} \{\ell(d, \theta_i)\} \right\} \end{aligned}$$

Consider aggregate losses over these three collections defined as

$$L_{D_i}(S) = \frac{1}{|D_i|} \sum_{d \in D_i} \min_{i \in S} \{\ell(d, \theta_i)\} \Rightarrow L_D(S) = \frac{1}{|D|} (|D_1|L_{D_1}(S) + |D_2|L_{D_2}(S) + |D_3|L_{D_3}(S))$$

Now, to show super-modularity of $L(S)$ it is sufficient to verify that for $i \in \{1, 2, 3\}$ we have

$$L_{D_i}(A) - L_{D_i}(A \cup \{j\}) \geq L_{D_i}(B) - L_{D_i}(B \cup \{j\}). \quad (2)$$

By construction $L_{D_3}(A) = L_{D_3}(A \cup \{j\})$ and $L_{D_3}(B) = L_{D_3}(B \cup \{j\})$, thus (2) holds for $i = 3$. Further, $L_{D_2}(B) = L_{D_2}(B \cup \{j\})$ and $L_{D_2}(A) \geq L_{D_2}(A \cup \{j\})$ due to monotonicity, therefore (2) holds for $i = 2$. For $i = 1$

- $L_{D_1}(A) = L_{D_1}(A \cup \{j\}) + |D|^{-1} \sum_{d \in D_1} (\min_{i \in A} \{\ell(d, \theta_i)\} - \ell(d, \theta_j))$
- $L_{D_1}(B) = L_{D_1}(B \cup \{j\}) + |D|^{-1} \sum_{d \in D_1} (\min_{i \in B} \{\ell(d, \theta_i)\} - \ell(d, \theta_j))$

Combining the two we get

$$L_{D_1}(A) - L_{D_1}(A \cup \{j\}) - L_{D_1}(B) + L_{D_1}(B \cup \{j\}) = |D|^{-1} \sum_{d \in D_1} \left(\min_{i \in A} \{\ell(d, \theta_i)\} - \min_{i \in B} \{\ell(d, \theta_i)\} \right) \geq 0$$

where the last inequality holds due to $A \subseteq B \Rightarrow \min_{i \in A} \{\ell(d, \theta_i)\} \geq \min_{i \in B} \{\ell(d, \theta_i)\}$. This confirms that (2) holds for $i = 1$ and concludes the proof. \square

Proof of Theorem 1. Similarly to Nemhauser et al. (1978), we prove by induction, however we slightly modify the invariant, which becomes

$$\forall i : L(\text{opt}) - L(S_i) \leq \left(1 - \frac{1 - \epsilon}{k}\right)^i L(\text{opt}),$$

where S_i is the set of items selected by the greedy algorithm after the i -th step, and opt is the optimal set of k items. It holds trivially for $i = 0$, thus we assume it holds for step $i - 1$ and prove the induction step. Let the marginal improvement be defined as $\ell_{S_{i-1}}(j) = L(S_{i-1} \cup \{j\}) - L(S_{i-1})$, then, by submodularity, for each $j \in \text{opt} \setminus S_{i-1}$ we have

$$\begin{aligned} L(S_{i-1} \cup (\text{opt} \setminus S_{i-1})) &= L(S_{i-1} \cup (\text{opt} \setminus S_{i-1} \setminus \{j\})) + \ell_{S_{i-1} \cup (\text{opt} \setminus S_{i-1} \setminus \{j\})}(j) \\ &\leq L(S_{i-1} \cup (\text{opt} \setminus S_{i-1} \setminus \{j\})) + \ell_{S_{i-1}}(j) \end{aligned}$$

Repeating the argument for all items $j \in opt \setminus S_{i-1}$ we obtain

$$L(S_{i-1} \cup (opt \setminus S_{i-1})) \leq L(S_{i-1}) + \sum_{j \in opt \setminus S_{i-1}} \ell_{S_{i-1}}(j)$$

And by monotonicity

$$L(opt) \leq L(S_{i-1} \cup (opt \setminus S_{i-1})) \leq L(S_{i-1}) + \sum_{j \in opt \setminus S_{i-1}} \ell_{S_{i-1}}(j) \quad (3)$$

It is easy to show by contradiction that the item j chosen at the i -th step has a marginal improvement

$$\ell_{S_{i-1}}(j) \geq \frac{1}{|opt \setminus S_{i-1}|} \sum_{\hat{j} \in opt \setminus S_{i-1}} \ell_{S_{i-1}}(\hat{j}) \geq \frac{1}{k} (L(opt) - L(S_{i-1}))$$

Where the last inequality follows from Equation 3. However, our theorem states that the greedy algorithm will only find a $(1 - \epsilon)$ approximation of the best marginal improvement, therefore

$$\ell_{S_{i-1}}(j') \geq \frac{1 - \epsilon}{k} (L(opt) - L(S_{i-1}))$$

Which we can use to prove the induction step

$$\begin{aligned} L(opt) - L(S_i) &= L(opt) - L(S_{i-1}) - \ell_{S_{i-1}}(j') \\ &\leq (L(opt) - L(S_{i-1})) - \frac{1 - \epsilon}{k} (L(opt) - L(S_{i-1})) \\ &\leq (L(opt) - L(S_{i-1})) \left(1 - \frac{1 - \epsilon}{k}\right) \leq \left(1 - \frac{1 - \epsilon}{k}\right)^i L(opt) \end{aligned}$$

This completes the proof by induction. Applying the induction invariant to the k -th step we obtain our desired result

$$L(opt) - L(S_k) \leq \left(1 - \frac{1 - \epsilon}{k}\right)^k L(opt) \leq e^{-1 + \epsilon} L(opt)$$

□

C Details of anytime HyperBand

Algorithm 3 contains the pseudo-code for our anytime HB algorithm. Note that in our case the term resource used in the HB algorithm corresponds to the number of datasets. We always set the minimal resource to be 1. Also, since we are choosing random datasets, this is a very crude but unbiased estimator of the mean. Querying a configuration with resource level r means taking the average of training jobs of the HP configuration over r datasets from our collection. We split the possible resource into *rungs*, in an exponential scale. That is, for rung $s = 0$, the resource level is $r = 1$, for $s = 1$, it is $r = \eta$ (default 3), for 2 it is $r = \eta^2$, until $s = s_{\max}$ for which it is $r = D$, the number of datasets. To avoid technical complications and cumbersome notations we simply assume D to be a power of η . Algorithm 3 describes the anytime HyperBand variant. Promoting a configuration to rung s means running the HP configuration on $r = \eta^s$ datasets, or rather $\eta^s - \eta^{s-1}$ if we account for information reuse, in order to get a better estimate of its true value. The algorithm will initially query configurations in rung 0, and when it can, it will promote configurations to larger rungs. Unlike the ASHA algorithm in Li et al. (2018), that is an anytime parallel implementation of the simpler successive halving algorithm, Algorithm 3 will once in a while choose not to promote a candidate from rung s to rung $s + 1$ but instead draw a new candidate and start it directly from rung $s + 1$. This is exactly the idea of HyperBand that overcomes issues with regions in the configuration space that are ‘unlucky’ in that they are misrepresented as high loss configurations when running with few resources. The exact ratio determining when a new configuration should be chosen rather than an old one to be promoted is set so that the overall resources used by each rung towards configurations that start in that rung (as opposed to being promoted to it) are equal. The expression of the ratio $\sum_{m=0}^{s-1} \frac{s_{\max} - s}{s_{\max} - m}$ in Algorithm 3 can be shown to provide an equal balance of resources. In other words, if we partition the configurations explored throughout the run of the algorithm according to

the first rung they were launched (these are called brackets in HB), the sum of resources used by the configurations in a partition in the rung they started in should be the same. Since this is a trivial exercise we do not prove it.

Algorithm 3: Anytime HyperBand

Input: Configuration Selector Θ , number of datasets D , elimination ratio η (default value 3)

Output: Configuration θ

$s_{\max} = \log_{\eta}(D)$;

for $t \in 1, 2, \dots$ **do**

for $s = s_{\max} - 1, s_{\max} - 2, \dots, 0$ **do**

if less than $1/\eta$ candidates in this rung s has been promoted **then**

 If we promoted over $\sum_{m=0}^{s-1} \frac{s_{\max}-s}{s_{\max}-m}$ items from rung s , reset the counter of number of promoted items from rung s , select a new configuration θ_{new} from Θ , and promote it to rung $s + 1$;

 Otherwise, promote the best performing candidate θ to rung $s + 1$;

end

end

 If no item was promoted above, select a new configuration θ_{new} from Θ and run it in rung 0;

 The best configuration θ at any time t is the one with the minimal loss among those that ran with the full resources

end

D HP search space

For the hyper parameters search spaces for XGBoost, LightGBM, CatBoost and MLP see Table 5. Our zero-shot AutoML (ZAML) meta-pipeline has the following structure. First, a simple heuristic is applied to detect the type of each column: columns with less than 20 unique values are treated as categorical, columns containing entries from the list of 500 most frequent English words treated as text, and the remaining columns that can be converted to numeric value are labeled as numeric. All ZAML configurations use TF-IDF with fixed hyper parameters for preprocessing text features. For numeric features ZAML first fills in missing values, then applies one of four preprocessors: quantile transform, binning, standard scaler or min-max scaler. For categorical features ZAML applies either one-hot or ordinal encoding. Finally one of three algorithms is used to train on the preprocessed data: XGBoost, LightGBM or MLP. The HP search space for ZAML meta-pipeline is presented in Table 5.

E Zero-shot HP configurations

We report the 5 zero-shot configurations for each setting in Tables 6-10. These were found by applying the Naive algorithm on the full table of training results. These configurations can be used by users of these algorithms as a simple yet effective way to perform hyperparameter tuning and reproduce the results reported in this paper.

F Datasets and generated tables.

All configurations were evaluated on the datasets listed in Table 11. These are datasets taken from the following public repositories: Kaggle⁴, OpenML (Vanschoren et al., 2013), UCI (Dua & Graff, 2017) and the AutoML Challenge (Guyon et al., 2019).

As mentioned in the main text, we split every dataset in ratios 50/25/25 for training, validation and test, respectively. Many datasets contain missing values and non-numeric inputs, in these cases we apply basic feature type detection (numeric, categorical and text) and preprocessing (one hot encoding for categorical features and TF-IDF for text features). For each of the five settings considered we then start N times D training jobs, by evaluating N randomly selected configurations on D datasets. See Table 1 for values of N and D .

⁴<https://kaggle.com>

For each setting we make the following files available⁵:

error_val.csv: miss-classification rate on the validation set, stored in a matrix M such that $M_{i,j}$ corresponds to the j -th dataset trained with the i -th configuration.

error_test.csv: miss-classification rate on the test set, stored in a matrix M such that $M_{i,j}$ corresponds to the j -th dataset trained with the i -th configuration.

configurations.json: a map from configuration index to the HPs of that configuration. Useful for training surrogate models.

datasets.json: mapping each dataset index to a dictionary containing the name and source of the dataset.

G Additional results

Tables 12-15 provide additional pairwise comparisons of the 4 zero-shot algorithms we tested. The RED in these tables is computed between the pair considered.

We also provide additional plots of the results reported in the main text (Figure 1 and 2). In all plots the RED for any given dataset is computed relative to the average test miss-classification rate of the 10 best configurations among all data we generated, selected by validation miss-classification rate. We plot the aggregate across all datasets, computed in a leave-one-dataset-out fashion. The shaded areas span one standard error in each direction, thus representing 68% confidence intervals of the mean. We refer to the caption of the images for additional details.

Figure 3 reports the result of an ablation study in which we compared the use of the average to that of the P90, when aggregating the meta-loss across all datasets. One reason one might be inclined to prefer the P90 is that it can be more robust to outliers and thus perform better on dataset dissimilar to those in our selection of datasets. However, our experiments show that using a P90 is unlikely to provide a benefit. Even if we are interested in the P90 (displayed in the second row of the figure) the zero-shot configurations computed using the average match – and in most cases outperform – the configurations computed by optimizing the P90.

Finally, Figure 4 shows the effect of the number of random configurations considered. These experiments show that considering more configurations does in fact allow us to compute better zero-shot configurations, thus providing a good argument in favour of more sample efficient zero-shot HPO algorithms.

⁵Link will be made available in future versions

Table 5: HP distributions.

Hyper parameter	Range	Distribution
XGBoost		
n_estimators	[4, 512]	log-uniform
learning_rate	$[10^{-6}, 1]$	log-uniform
gamma	$[2^{-20}, 64]$	log-uniform
min_child_weight	[1, 32]	log-uniform
max_depth	[2, 32]	log-uniform
reg_lambda	$[2^{-20}, 1]$	log-uniform
reg_alpha	$[2^{-20}, 1]$	log-uniform
subsample	[0.5, 1]	uniform
colsample_bytree	[0.3, 1]	uniform
LightGBM		
boosting_type	['gbdt', 'dart', 'goss']	uniform
subsample	[0.5, 1]	uniform
num_leaves	[30, 150]	uniform
learning_rate	[0.01, 0.1]	log-uniform
subsample_for_bin	[20000, 30000]	uniform
min_child_samples	[20, 500]	uniform
reg_alpha	[0, 1]	uniform
reg_lambda	[0, 1]	uniform
colsample_bytree	[0.6, 1]	uniform
CatBoost		
iterations	[10, 100]	uniform
depth	[1, 8]	uniform
learning_rate	[0.01, 1]	log-uniform
random_strength	$[10^{-9}, 10]$	log-uniform
bagging_temperature	[0, 1]	uniform
border_count	[1, 255]	uniform
l2_leaf_reg	[2, 30]	uniform
MLP		
batch_size	$[2^4, 10^9]$	log_uniform
lr	$[10^{-4}, 10^{-1}]$	log_uniform
weight_decay	$[10^{-5}, 10^{-1}]$	log_uniform
max_units	$[2^6, 2^{10}]$	log_uniform
momentum	[0.1, 0.9]	uniform
num_layers	[1, 5]	uniform
max_dropout	[0.1, 0.99]	uniform
use_dropout	[False, True]	uniform
activation	["relu"]	fixed
n_epochs	[100]	fixed
ZAML		
categorical_preprocessor	["ordinal", "onehot"]	uniform
numeric_preprocessor	["quantile", "kbins", "standard", "minmax"]	uniform
algorithm	["MLP", "XGBoost", "LightGBM"]	uniform
kbins_nbins	$[2^4, 2^8]$	log_uniform
kbins_encode	["onehot", "ordinal"]	uniform
quantile_n_quantiles	[10, 1000]	log_uniform
xgb_hps	see above	
mlp_hps	see above	
lgb_hps	see above	

Table 6: Zero-shot configurations found for XGBoost.

	zero-shot ₀	zero-shot ₁	zero-shot ₂	zero-shot ₃	zero-shot ₄
colsample_bytree	6.19e-01	8.4e-01	3.88e-01	8.79e-01	9.86e-01
gamma	9.46e-05	7.04e-03	1.55e-05	8.43e-04	2.25e-05
learning_rate	6.74e-02	6.76e-02	9.74e-02	4.98e-03	3.57e-01
max_depth	7	3	18	9	20
min_child_weight	1	1	1	1	1
n_estimators	450	498	348	320	187
reg_alpha	3.69e-01	1.08e-04	6.57e-02	4.46e-03	2.97e-01
reg_lambda	6.08e-04	2.09e-05	1.05e-06	2.16e-04	3.8e-01
subsample	8.29e-01	9.7e-01	5.25e-01	8.38e-01	9.04e-01

Table 7: Zero-shot configurations found for LightGBM.

	zero-shot ₀	zero-shot ₁	zero-shot ₂	zero-shot ₃	zero-shot ₄
boosting_type	gbdt	goss	gbdt	goss	dart
colsample_bytree	9.28e-01	9.38e-01	6.98e-01	8e-01	7.74e-01
learning_rate	9.47e-02	9.8e-02	8.86e-02	9.99e-02	2.71e-02
min_child_samples	27	57	21	34	21
num_leaves	149	35	101	92	120
reg_alpha	6.7e-02	3.99e-02	2.13e-01	4.49e-02	5.41e-01
reg_lambda	7.22e-01	1.13e-01	7.3e-01	2.3e-01	2.56e-01
subsample	9.8e-01	8.65e-01	8.18e-01	6.34e-01	6.1e-01
subsample_for_bin	79750	106441	178491	272642	264651

Table 8: Zero-shot configurations found for CatBoost.

	zero-shot ₀	zero-shot ₁	zero-shot ₂	zero-shot ₃	zero-shot ₄
bagging_temperature	9.4e-01	3.56e-01	9.21e-01	6.56e-01	7.12e-01
border_count	223	92	250	65	76
depth	7	6	4	7	7
iterations	714	992	837	870	92
l2_leaf_reg	2	2	11	2	4
learning_rate	2.2e-01	1.75e-01	7.16e-02	1.88e-01	2.51e-02
random_strength	6.17e-05	4.08e-02	4.93e+00	1.72e+00	6.41e-08

Table 9: Zero-shot configurations found for MLP.

	zero-shot ₀	zero-shot ₁	zero-shot ₂	zero-shot ₃	zero-shot ₄
batch_size	165	63	32	28	17
lr	4.51e-02	1.3e-02	5.35e-02	7.77e-02	8.86e-02
max_dropout	9.35e-01	3.54e-01	4.87e-01	3.71e-01	2.53e-01
max_units	982	85	775	871	790
momentum	8.86e-01	9.08e-01	8.75e-01	1.67e-01	8.18e-01
num_layers	3	2	4	4	4
use_dropout	False	False	False	False	False
weight_decay	4.3e-04	2.89e-03	3.21e-05	3.3e-05	1.19e-04

Table 10: Zero-shot configurations found for ZAML.

	zero-shot ₀	zero-shot ₁	zero-shot ₂	zero-shot ₃	zero-shot ₄
algo	xgb	mlp	xgb	mlp	xgb
categorical	onehot	onehot	onehot	onehot	onehot
kbins_encode	onehot	ordinal	ordinal	ordinal	onehot
kbins_n_bins	40	93	99	31	17
numeric	quantile	minmax	minmax	standard	quantile
quantile_n_quantiles	822	236	296	12	24
mlp_batch_size	–	64	–	23	–
mlp_lr	–	9.67e-02	–	4.53e-02	–
mlp_max_dropout	–	8.e-01	–	8.85e-01	–
mlp_max_units	–	460	–	978	–
mlp_momentum	–	7.6e-01	–	9.56e-01	–
mlp_num_layers	–	3	–	4	–
mlp_use_dropout	–	False	–	False	–
mlp_weight_decay	–	1.81e-05	–	8.e-05	–
xgb_colsample_bytree	5.52e-01	–	6.94e-01	–	8.11e-01
xgb_gamma	7.51e-04	–	8.82e-01	–	7.13e-06
xgb_learning_rate	2.8e-01	–	3.73e-02	–	1.31e-06
xgb_max_depth	5	–	16	–	6
xgb_min_child_weight	2	–	2	–	1
xgb_n_estimators	195	–	94	–	252
xgb_reg_alpha	5.23e-05	–	1.03e-03	–	1.11e-04
xgb_reg_lambda	3.33e-06	–	2.35e-06	–	1.84e-06
xgb_subsample	8.76e-01	–	9.18e-01	–	8.97e-01

Table 11: Datasets.

UCI: Abalone, Avila, BankMarketing, BlogFeedback, ChessKingRookvsKing, ConditionBasedMaintenanceofNavalPropulsionPlants, DatasetforSensorlessDriveDiagnosis, Diabetes130UShospitalsforyears19992008, Dota2GamesResults, ElectricalGridStabilitySimulatedData, FacebookCommentVolumeDataset, Gisette, HTRU2, IDA2016Challenge, InsuranceCompanyBenchmarkCOIL2000, InternetAdvertisements, LetterRecognition, MoCapHandPostures, Nursery, OnlineShoppersPurchasingIntentionDataset, ParkinsonsTelemonitoring, PenBasedRecognitionofHandwrittenDigits, PhysicalUnclonable, PhysicochemicalPropertiesofProteinTertiaryStructure, PokerHand, SGEMMGPUkernelperformance, Spambase, StatlogLandsatSatellite, SuperconductivityData, TurkiyeStudentEvaluation, UJIIndoorLoc, p53Mutants, WeightLiftingExercisesmonitoredwithInertialMeasurementUnits, YearPredictionMSD

AutoML Challenge: adult, albert, cadata, christine, digits, dilbert, dionis, fabert, helena, jannis, madeline, philippine, robert, sylvine, volkert, yolanda

Kaggle: blastchar/telco-customer-churn, burakhmmtgl/energy-molecule, lplisallerl/air-tickets-between-shanghai-and-beijing, greenwing1985/housepricing, harlfoxem/housesalesprediction, jsphyg/weather-dataset-rattle-package, lodetomasi1995/income-classification, loveall/appliances-energy-prediction, contactprad/bike-share-daily-data, muonneutrino/us-census-demographic-data, olgabelitskaya/classification-of-handwritten-letters, shrutimechlearn/churn-modelling, umairmsr87/predict-the-number-of-upvotes-a-post-will-get

OpenML: wilt (40983), mfeat-morphological (18), ozone-level-8hr (1487), sick (38), jm1 (1053), mfeat-fourier (14), har (1478), churn (40701), phoneme (1489), wall-robot-navigation (1497), numerai28.6 (23517), isolet (300), mfeat-pixel (40979), first-order-theorem-proving (1475), mfeat-factors (12), kc1 (1067), mnist_784 (554), GesturePhaseSegmentationProcessed (4538), electricity (151), texture (40499), jungle_chess_2pcs_raw_endgame_complete (41027), PhishingWebsites (4534), mfeat-karhunen (16), Bioresponse (4134), connect-4 (40668), segment (40984), mfeat-zernike (22), steel-plates-fault (40982), Fashion-MNIST (40996), nomao (1486), splice (46), dna (40670), madelon (1485),

Table 12: OBO (vs MF) – avg RED (\pm std. err.) – lower is better.

	1 zero-shot config	2 zero-shot configs	5 zero-shot configs
XGBoost	-2.44% (\pm 0.87)	-2.78% (\pm 0.79)	-2.75% (\pm 0.64)
LightGBM	-4.37% (\pm 1.41)	-4.72% (\pm 1.38)	-4.68% (\pm 1.32)
CatBoost	-3.32% (\pm 0.98)	-1.47% (\pm 0.79)	-2.24% (\pm 0.90)
MLP	-1.52% (\pm 1.50)	-2.01% (\pm 1.20)	-1.46% (\pm 1.40)
ZAML	-0.15% (\pm 2.64)	+1.68% (\pm 2.49)	+0.18% (\pm 2.66)
Combined	-2.70% (\pm 0.63)	-2.35% (\pm 0.58)	-2.57% (\pm 0.59)

Table 13: Surrogate (vs Naive) – avg RED (\pm std. err.) – lower is better.

	1 zero-shot config	2 zero-shot configs	5 zero-shot configs
XGBoost	-1.98% (\pm 1.87)	-3.09% (\pm 1.81)	-4.15% (\pm 1.75)
LightGBM	-7.42% (\pm 1.76)	-6.46% (\pm 1.67)	-6.67% (\pm 1.62)
CatBoost	+0.04% (\pm 1.82)	+0.61% (\pm 1.72)	+0.99% (\pm 1.65)
MLP	+6.04% (\pm 3.05)	-0.11% (\pm 1.36)	-2.68% (\pm 1.33)
ZAML	-0.36% (\pm 2.34)	+1.53% (\pm 1.89)	-0.81% (\pm 1.75)
Combined	-1.38% (\pm 0.98)	-2.11% (\pm 0.80)	-3.06% (\pm 0.77)

Table 14: MF (vs Surrogate) – avg RED (\pm std. err.) – lower is better.

	1 zero-shot config	2 zero-shot configs	5 zero-shot configs
XGBoost	-2.90% (\pm 0.81)	-2.11% (\pm 0.78)	-0.16% (\pm 0.67)
LightGBM	+3.66% (\pm 1.35)	+3.16% (\pm 1.27)	+3.54% (\pm 1.25)
CatBoost	+2.22% (\pm 1.27)	+1.35% (\pm 1.04)	+1.08% (\pm 1.07)
MLP	-5.70% (\pm 3.24)	-1.17% (\pm 1.77)	+0.59% (\pm 1.56)
ZAML	+1.38% (\pm 3.58)	-0.44% (\pm 3.34)	+1.75% (\pm 3.02)
Combined	-0.09% (\pm 0.87)	+0.35% (\pm 0.67)	+1.42% (\pm 0.62)

Table 15: OBO (vs Naive) – avg RED (\pm std. err.) – lower is better.

	1 zero-shot config	2 zero-shot configs	5 zero-shot configs
XGBoost	-7.21% (\pm 1.90)	-7.96% (\pm 1.85)	-7.14% (\pm 1.82)
LightGBM	-7.69% (\pm 1.75)	-6.92% (\pm 1.68)	-7.33% (\pm 1.64)
CatBoost	-1.87% (\pm 1.17)	-0.60% (\pm 1.15)	-1.40% (\pm 0.84)
MLP	-2.85% (\pm 2.01)	-3.47% (\pm 1.57)	-2.78% (\pm 1.84)
ZAML	-2.77% (\pm 3.48)	-2.90% (\pm 3.32)	-3.52% (\pm 3.04)
Combined	-4.92% (\pm 0.88)	-4.75% (\pm 0.83)	-4.78% (\pm 0.80)

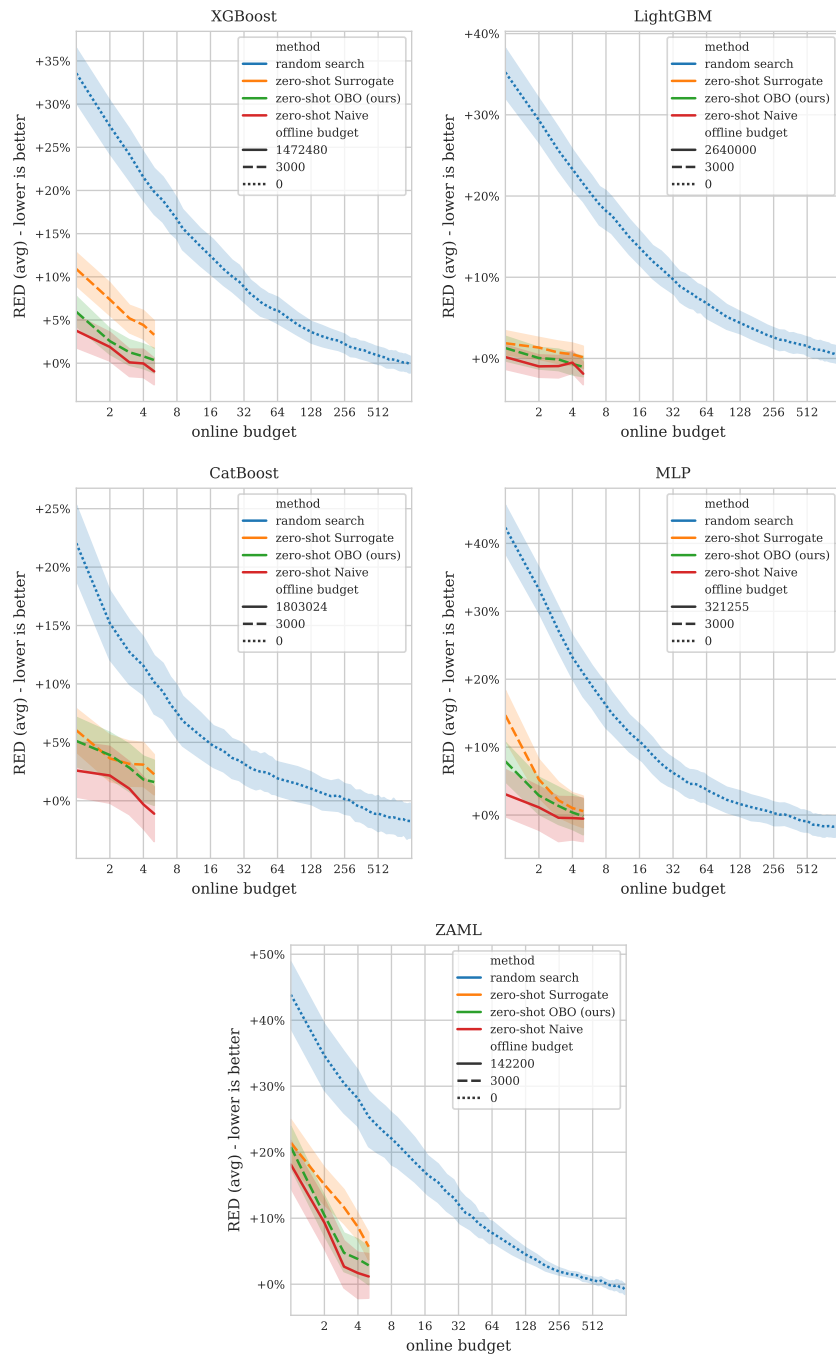


Figure 1: **Results for OBO.** Performance obtained by performing HPO using zero-shot configurations found by OBO (green). We compare the performance with the baseline (red) corresponding to zero-shot configurations computed applying the naive algorithm on all the data we have available (note the orders of magnitude more training jobs used to find these configurations), and Surrogate (orange), the best performing existing efficient method. For comparison we also include the performance of random search, which does not require any offline training, but as expected requires a much larger online budget to find competitive HP configurations.

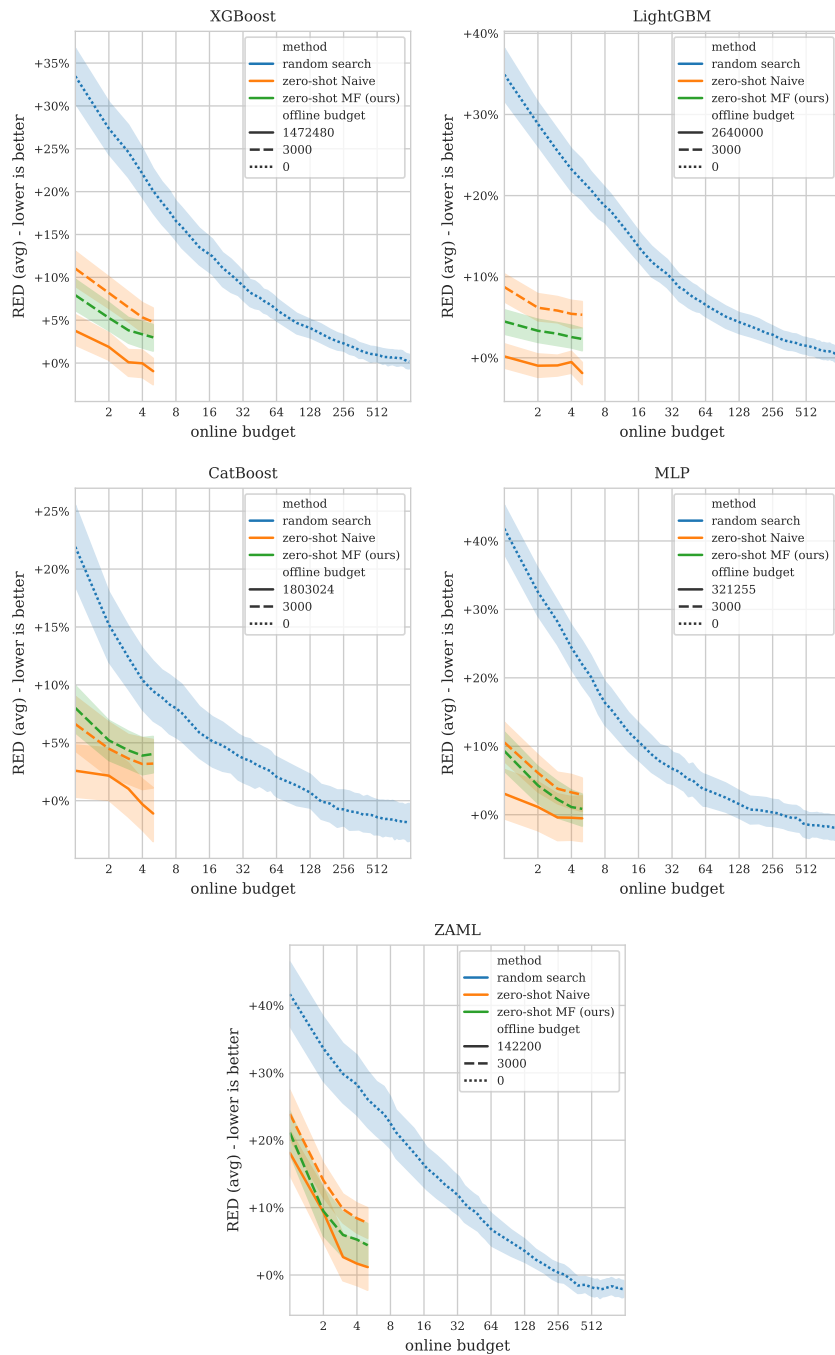


Figure 2: **Results for MF.** Performance obtained by performing HPO using zero-shot configurations found by our multi-fidelity algorithm (green). We compare the performance with the Naive baseline (orange) applied to all the data we have available (note the orders of magnitude more training jobs used to find these configurations) and on a randomly sub-sampled table using the same offline budget as the multi-fidelity algorithm. For comparison we also include the performance of random search, which does not require any offline training, but as expected requires a much larger online budget to find competitive HP configurations.

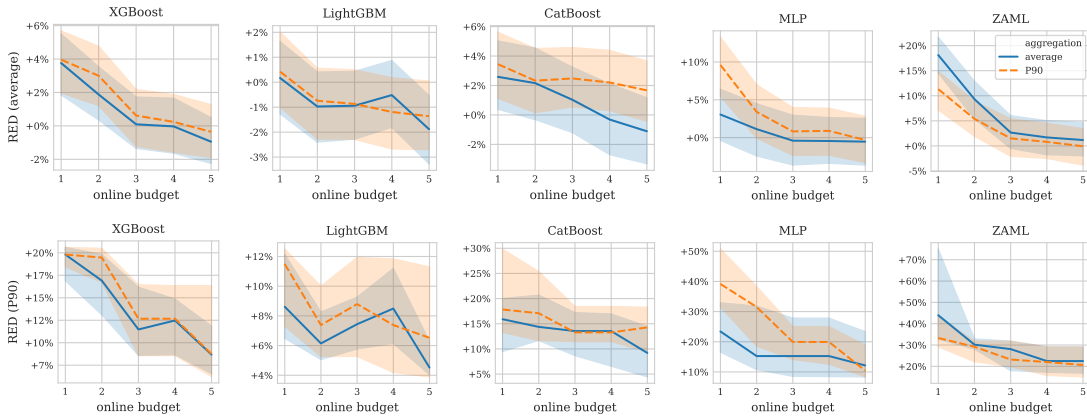


Figure 3: **Ablation study: aggregation.** These plots compare the use of the **average** (blue) with the use of the **P90** (orange) when aggregating the meta-loss among different datasets. The top row shows the average performance of the zero-shot configurations found using the two strategies, while the bottom row shows the P90 across the datasets, with bootstrapped confidence intervals.

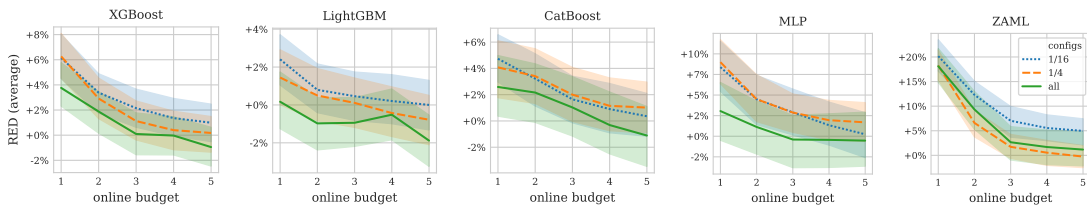


Figure 4: **Ablation study: number of configurations.** These plots show the effect of reducing the number of configurations considered. In all cases we use the Naive algorithm. We can see that in general using the full data we generated (green) provides better zero-shot configurations than using 1/4th of the data (orange) and 1/16th of the data (blue).